JOURNAL OF SOLID STATE CHEMISTRY **131,** 221–230 (1997)
ARTICLE NO. SC977359

The Phases of the Antifluorite Deuterated-Ammonium Palladium Hexachloride, $(ND_4)_2PdCl_6$

I. P. Swainson,* B. M. Powell,* and R. D. Weir†

*Neutron and Condensed Matter Science, Atomic Energy of Canada Limited, Chalk River Laboratories, Chalk River, Ontario, K0J 1J0, Canada; and †Department of Chemistry and Chemical Engineering, Royal Military College of Canada, Kingston, Ontario, K7K 5LO, Canada

Received June 17, 1996; in revised form December 2, 1996; accepted February 20, 1997

A structural phase transition occurs at $T_c = 30.2 \pm 0.1$ K in the deuterated antifluorite $(ND_4)_2PdCl_6$, but not in its protonated analogue, and shows the largest transition entropy of all the deuterated ammonium hexachlorides. The structure of the antifluorite $(ND_4)_2PdCl_6$ has been studied at room temperature and at 5 K using neutron powder diffraction. The data taken at room temperature show strong evidence for disorder of the ND_4 molecule. The space group of the compound at 5 K is shown to be $P2_1/n$. The major change in the structure during this isotopically induced transition is a large rotation of the ND_4 ions, with relatively little change in the orientation of the $PdCl_6$ units. A comparison to previous calorimetric and inelastic neutron scattering studies of the compound leads to the conclusion that the ND_4 ions dominate the transition entropy and inelastic spectrum of $(ND_4)_2PdCl_6$.

INTRODUCTION

Antifluorites are described by the general formula R_2MX_6, in which R may be an alkali metal or ammonium ion and MX_6 represents a metal halide octahedron, with a wide variety of chemical compositions. At high temperatures, all antifluorites crystallize in the cubic $Fm\bar{3}m$ space group. At lower temperatures many antifluorites show phase transitions to lower-symmetry structures. There have been extensive studies of many of these transitions over recent years (e.g. (1–5)). A common feature of alkali metal antifluorite transitions is that the MX_6 octahedra show coupled rotations and/or translations. The phase transitions can be modelled assuming soft MX_6 external modes as the driving forces for transition. There is strong evidence for this from inelastic neutron scattering measurements (6–8).

With ammonium ions present, extra degrees of orientational freedom arise. This raises the possibility of coupling between the orientational degrees of freedom of the ammonium and octahedral external modes. For ammonium antifluorites, the soft mode is likely to be one that does not significantly distort either the ammonium or metal halide units. The relationship between the various instabilities in the ammonium antifluorites, the size of the unit cell, and the composition of the MX_6 unit has been discussed recently by Zhang *et al.* (9). There is some suggestion that transitions additional to those predicted from group–subgroup relationships can be generated in these systems, provided that the transition can happen continuously (the nondisruptive criterion) (10, 11). This may explain some unusual increases in symmetry at low temperatures in certain antifluorites with more than one transition (11, 12).

A further intriguing feature of the ammoniated antifluorites is that certain of them, e.g., $(ND_4)_2PdCl_6$ (13, 14), $(ND_4)_2PtCl_6$ (15–17), $(ND_4)_2PbCl_6$ (18), $(ND_4)_2SeCl_6$ (19, 20), and $(ND_4)_2TeCl_6$ (12, 21–23), show structural phase transitions only in the deuterated forms. This has been demonstrated using adiabatic calorimetric measurements of these compounds (13–16, 21–23), showing that the interactions of the ammonium ion with the MX_6 units are a great influence on the stability of the cubic phase. $(ND_4)_2TeCl_6$ has been the subject of comprehensive study of the complicated series of phase transitions seen on cooling from room temperature, some of which show some apparent increases in symmetry (12).

In general, the larger the alkali ion, R, is, the more the cubic phase is stabilized at the expense of any competing lower symmetry distortions (24). An explanation for the origin of the isotopically induced phase transitions has been forwarded by Kume *et al.* (12). At high temperatures, the rotational disorder of the ammonium ion means that it resembles a spherical ion. The radius of the ammonium ion is relatively large and close to that of K^+, and ammonium antifluorites are, therefore, fairly stable in the cubic phase (24). As the moment of inertia of NH_4^+ is lower than that of ND_4^+, its rotational wave function is angularly more delocalized, and even at low temperatures will still resemble a large spherical alkali ion, and this suppresses the possibility of the formation of lower symmetry phases.

In the case of $(ND_4)_2PdCl_6$, the subject of this study, the transition temperature has been measured as 30.2 ± 0.1 K (14). It has been suggested previously that the low-temperature

0022-4596/97 $25.00

phase of $(ND_4)_2PdCl_6$ is tetragonal (6), but no details were supplied. This study examines the low-temperature structure in detail and, surprisingly, appears to be the first refinement to report the orientation of the ammonium ions in a low-temperature phase of an antifluorite.

EXPERIMENTAL

A powdered sample of $(ND_4)_2PdCl_6$ was provided by Dr. M. Prager, Institut für Festköpforschung, Jülich, Germany. This sample has been used previously in an inelastic neutron scattering study (6) and calorimetric measurements (14). The samples were ground and loaded into a vanadium can of diameter 5 mm under a helium exchange gas. The can was placed in a helium cryostat for measurement at 5 K. Neutron powder diffraction experiments were performed at the NRU reactor operated by AECL, Chalk River, using the C2 DUALSPEC powder diffractometer. The instrument consists of an 800 wire detector spanning 80° 2θ. The experiment used a wavelength of 1.7065 (3) Å which was calibrated using a separate Si reference powder. An incident beam of collimation 0.4° was used with a Si(115) monochromator. Diffraction patterns were measured at room temperature and at 5 K (with a stability of $\pm$ 1 K). The conditions for the refinements presented in this paper are shown in Table 1.

The data were refined using the Rietveld code of the GSAS suite of programs (25). The lineshape used was that of the standard GSAS pseudo-Voigt function with coupled asymmetry. Data at room temperature were fitted in the cubic space group $Fm\bar{3}m$. The refinements were all constrained as rigid body refinements, assuming perfect tetrahedral and octahedral shapes for the ND_4 and $PdCl_6$ units, respectively. Temperature factors were refined as TLS tensors, but as a further constraint, to reduce the number of refineable parameters, the translations (T) and librations (L) were assumed to be isotropic in the low-temperature phase, an approximation we justify on the basis of the relatively small distortion from the cubic supergroup. A number of space groups have been reported previously for antifluorites at low temperatures. For the 5 K data, these were evaluated on the basis of their fit to the observed splittings and superlattice peaks. For all refinements an absorption correction of 0.92 cm^{-1} was applied, due to the appreciable absorption cross section of Cl.

TABLE 1
Refinement Conditions for the Four Structure Refinements Presented

	Ordered $Fm\bar{3}m$	Disordered $Fm\bar{3}m$	$C2/c$	$P2_1/n$
λ/ Å	1.7065 (3)	1.7065 (3)	1.7065 (3)	1.7065 (3)
2θ range/°	15–120	15–120	15–119	15–119
$\Delta 2\theta$/°	0.05	0.05	0.05	0.05
μ (cm^{-1})	0.92	0.92	0.92	0.92
Weighted profile, R_{wp}/%	8.02	6.08	7.38	5.68
Expected, R_{ex}/%	3.02	3.02	3.01	3.01
Profile, R_p/%	5.85	4.51	5.57	4.16
χ^2	7.13	4.08	6.11	3.63
# Observations, N	2094	2106 (12 soft)	2078	2078
# Parameters, P	18	22	41	43
# distinct hkl	44	44	522	522

$$R_{wp} = \sqrt{\sum w(y_{obs} - y_{cal})^2 / \sum w y_{obs}^2}$$
$$R_{ex} = \sqrt{[N - P] / \sum y_{obs}^2}$$
$$R_p = \sum |y_{obs} - y_{cal}| / \sum y_{obs}$$
$$\chi^2 = R_{wp}^2 / R_{ex}^2$$

Refinement of Room Temperature Data

In $Fm\bar{3}m$, the $PdCl_6$ octahedral faces lie in $\{111\}$. A choice exists for the orientation of the ND_4 tetrahedra. The N–D vectors may point parallel to the normal of the octahedral faces (the "normal" orientation), so that the base of the tetrahedron is adjacent to an octahedral face, or they may point in the "inverted" orientation, so that the N–D vectors (and the apices of the tetrahedron) point directly toward the octahedral faces.

The results of the refinement of the room temperature diffraction pattern with the ND_4 molecule in the "normal" orientation are shown in Table 2. The fit is displayed in Fig. 1 and gave a χ^2 of 7.13. For comparison a refinement was performed in which the ND_4 ion was in the inverted orientation. The χ^2 for such a fit was significantly higher at 20.7. This shows that the gross direction of preferred orientation for ND_6 is the 'normal" orientation, and this agrees with previous findings in the cubic phases of the protonated ammonium antifluorites $(NH_4)_2SnBr_6$ (1), $(NH_4)_2PtBr_6$ (2), $(NH_4)_2PbCl_6$ (3), and $(NH_4)_2TeCl_6$ (26).

In addition to the Bragg peaks due to $Fm\bar{3}m$ (O_h^5), some very weak impurity peaks were found at 36.5°, 39.4°, 56.8°, and 69.4° 2θ. These were not excluded from the patterns

TABLE 2
Structural Parameters for $(ND_4)_2PdCl_6$ at Room Temperature, Refined as $Fm\bar{3}m$ (O_h^5), with ND_4 Molecules in the "Normal" Orientation

a/Å						V/Å^3
9.7262(3)						920.08(9)
	x	y	z	T/Å^2	L/°^{2}	U_{iso}/Å^2
Pd	0	0	0	0.0191(5)		0.0191
Cl	0.2392(2)	0.0000	0.0000	0.0191(5)	1.3(5)	0.0205
N	0.2500	0.2500	0.2500	0.0318(5)		0.0318
D	0.3109(2)	0.3109(2)	0.3109(2)	0.0318(5)	420(3)	0.1214
Body						Bond/Å
ND_4						1.025
$PdCl_6$						2.327(2)

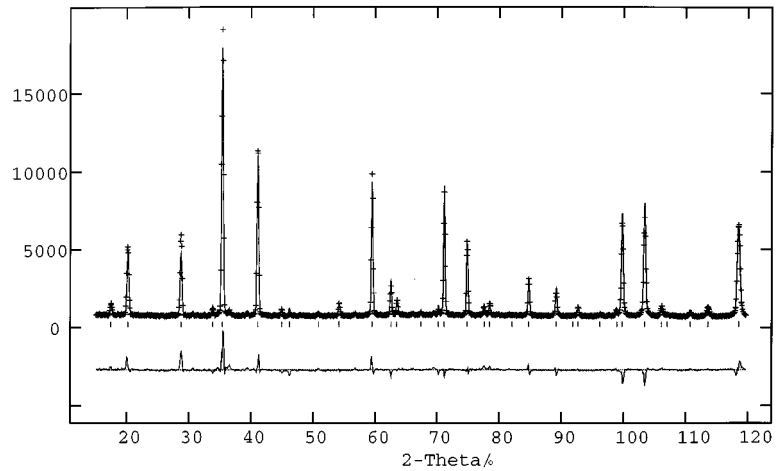

FIG. 1. Observed (points) diffraction pattern of $(ND_4)_2PdCl_6$ at room temperature, fitted (lines) using an ordered ND_4 model.

during the fits. An attempt was made to refine the ND_4 molecule as being ordered along the "normal" [111] direction. The assumption was made for the refinements that the ND_4 and $PdCl_6$ were undeformable rigid bodies of perfect tetrahedral and octahedral symmetry, respectively. This is justified by the knowledge that any soft modes are primarily external molecular modes. The N–D bond length was fixed at 1.025 Å, the mean value seen in ammonium compounds (27). The value of the Pd–Cl bond length was left as a variable parameter. In GSAS, the rigid bodies are set up in a Cartesian environment and the rigid body axes XYZ are related to the cell axes abc by $X \parallel a$, $Z \parallel a \times b$, and $Y \parallel (a \times b) \times a$ (25). TLS tensors were used to describe the molecular motion for both ND_4 and $PdCl_6$ units. Both molecules are on sites that are of sufficiently high symmetry that there is only one translational and one librational coefficient. In $PdCl_6$, the librational component refined to be almost zero. The same effect was obtained both with and without absorption corrections and when the Pd–Cl bond length was varied or fixed at the values determined from the 5 K monoclinic refinements.

We note that the orientation of the ND_4 molecule in $(ND_4)_2SeCl_6$ has been studied previously (19). These authors showed that a significant proportion of the orientational distribution of the ND_4 tetrahedron is tilted off-axis in $(ND_4)_2SeCl_6$. Fig. 1 shows that appreciable systematic errors are present in the refinement of the $(ND_4)_2PdCl_6$ data, when the ND_4 molecules are ordered along the "normal" orientation. To improve the fit, several different refinements were performed that allowed the ND_4 molecules to move off-axis from the "normal" orientation.

In the first set of refinements, the D atoms were set on the 96*k* sites with 1/3 occupancy and the N–D bond lengths were subject to soft (slack) constraints. The weighting of these constraints was varied to examine the sensitivity of the refinement to the weighting procedure: starting from a basically unconstrained model with zero weight, the constraint weight was increased in powers of 10 to one approaching a rigid bond refinement with a weight of 1000. The N–D bond length was soft constrained to 1.025 (2) Å, the mean value reported from other ammonium salts (27). As the weight was increased, the bond lengths necessarily approached their constrained values. For those models with a nonzero weight, the refined angle between the N–D bond vector and the [111] direction remained approximately independent of weight ($19 \pm 1^\circ$). This gives us confidence in the physical reality of the N–D off-axis tilt in this system. In addition, the N and D Debye–Waller factors were relatively weight-independent, showing only a slow variation (increase for N, decrease for D) with increasing weight, with all the changes being within one refined esd from a unit weighting to a weight of 1000. Soft constraint refinements were performed where the D atom fractionally occupied the general equivalent positions, 192*l* sites, but these proved to be unstable. A similar instability was reported when this was attempted in the refinement of $(ND_4)_2SeCl_6$ (19). It is likely that the D atoms are not strongly localized at the 92*k* sites, since we might expect the 192*l* refinements to "lock in" to 92*k* sites if this were the case.

The soft constraint model, while permitting the off-axis tilt of the N–D bond does not preserve the shape of the ND_4 tetrahedron, and the D–N–D internal angles are substantially distorted by the operations of the N site symmetry ($\bar{4}3m$). Rigid body refinements were also attempted to preserve the ideal tetrahedral shape of the ND_4 molecule, while allowing for off-axis motion. Such a refinement necessitates the D atoms sitting on 192*l* sites. This 192*l*-refinement was as unstable to refinement when all degrees of rotational freedom were allowed, as the soft constraint models were when the D atoms occupied these sites. Because of the

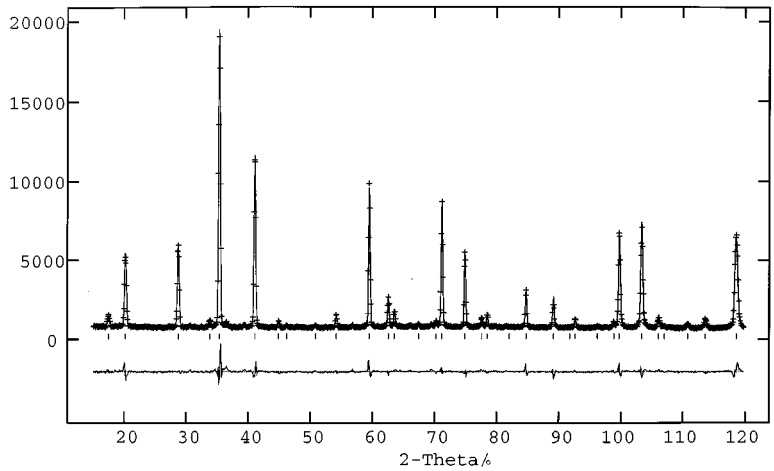

FIG. 2. Observed (points) diffraction pattern of $(ND_4)_2PdCl_6$ at room temperature, fitted (lines) using a disordered ND_4 model, with partial occupancy of the 96*k* sites.

unsatisfactory performance of the rigid body refinements of the disordered D nuclear density distribution, we do not present these refinements here.

In the soft constrained refinements, because of the weight-independence of the refined angular deviation of the N–D vector from [111], we present the disordered refinement of the cubic phase, in which we used a soft constraint weight of 1000. The fit is depicted in Fig. 2. A comparison to Fig. 1 shows that the systematic errors in the fit are substantially reduced in this model, and the χ^2 drops from 7.13, in the ordered phase, to 4.19.

Both soft constraints, and rigid body refinements of this disorder are discrete approximations to what is probably a continuous dynamic distribution of nuclear density, which may or may not be partly localized near the 96*k* sites. Due to the distortion of the ND_4 molecule in the soft constrained model, presented in Fig. 2 and Table 3, care should be taken in the interpretation of the refined D positions. Due to the strong weighting of the soft constraint on the N–D bond length in the presented refinement, we are fairly certain that the D atoms lie on the correct radius to model the nuclear density distribution traced out by N–D motion. We believe that this refinement is the best approximation to the N–D disorder that can be achieved using standard Rietveld methods. We, therefore, present the D positions only as a guide to the approximate angular deviation of the N–D vector from [111].

Refinements of 5 K Data

There have been many previously reported structures of antifluorites at low temperatures, which have been refined in tetragonal, trigonal, and monoclinic space groups. The method generally used is one of trial and error, where every possible subgroup is tested after logically excluding as many subgroups as possible. Certain peaks such as the 400 cubic line split in a ratio of approximately 2:1, characteristic of a tetragonal distortion. The trigonal (rhombohedral) system could be rejected on the basis of the observed peak splittings.

If the transition is driven by a Γ-point external mode of $PdCl_6$, the possible low-temperature space groups have been listed in Table 2 of (11). Rhombohedral space groups were ruled out on the basis of the observed peak splittings of certain peaks. Space group $C2/m$ was found to give a poor

TABLE 3

Structural Parameters for $(ND_4)_2PdCl_6$ at Room Temperature, Refined as $Fm\bar{3}m$ (O_h^5), with Disordered ND_4 Molecules on 96*k* sites with N–D bonds Soft Constrained to 1.025(2) Å, and a Weight of 1000

a/ Å					V/Å^3
9.7264(2)					920.13(7)
Atom	*x*	*y*	*z*	U_{eqv}/Å^2	
Pd	0	0	0	0.0190(5)	
Cl	0.2392(2)	0.0000	0.0000	0.0190(5)	
N	0.2500	0.2500	0.2500	0.0256(9)	
D	0.3109(2)	0.3109(2)	0.3109(2)	0.050(2)	
Deuterium anisotropic Debye–Waller factors					
U_{11}	U_{22}	U_{33}	U_{12}	U_{23}	U_{13}
0.011(2)	0.070(2)	0.070(2)	0.008(1)	0.008(1)	−0.033(2)
Molecule		Status			Bond/Å
ND_4		Slack			1.0249(2)
$PdCl_6$		Free			2.32(2)

fit also. For $I4/m$ (C_{4h}^5), the lowest symmetry tetragonal space group, the most obvious absence is that of the doublet near 120°, however, other weaker superlattice peaks are missing, e.g., around 30.6°, 47.5°, and 79.6° 2θ. The 30.6° reflection can be indexed as 201 on a cubic/pseudo-cubic lattice and is symmetry forbidden for all such I-centered lattices. As all the possible Γ-point tetragonal space groups are I-centered the zone center tetragonal space groups could all be ruled out. Furthermore, the space group $Fmmm$ which has recently been suggested by Kume and Asaji (17) for the low temperature phase of $(ND_4)_2PtCl_6$ on the basis of ^{35}Cl NQR cannot hold for the Pd-analogue for the same reasons.

Next the X-point instabilities were investigated. The likely subgroups are again external modes of the $PdCl_6$ octahedra. Possible space groups have been shown to be $Pnnm$ (D_{2h}^{12}), $P4/mnc$ (D_{4h}^6) and $P4_2/nmc$ (D_{4h}^{15}). Of these only $P4/mnc$ showed a reasonable fit to the data with a χ^2 of 10.54, R_p of 7.29% and R_{wp} of 9.83%. The ND_4 groups are free to rotate only about Y in this space group. The N–D bond length refined in this space group was 0.935 Å, which is rather short (27). Three are still some observed reflections that are not generated by this structure, e.g., the peak at 30.6°. It appears that the n-glide parallel to (100) could not be present. As there is no evidence for any doubling of the unit cell edges revealed by the new low-temperature peaks, it was decided to examine the Γ-point subgroups of $P4/mnc$ (D_{4h}^6).

The potential Γ-point instabilities of $P4/mnc$ are given by Stokes and Hatch (28). Of these $Pnnm$, $P4nc$, $P\bar{4}n2$, and $Pmn2_1$ could be immediately rejected on the basis of systematic absences. This leaves $P4/m$, $P42_12$, $P\bar{4}2_1c$, $Cccm$, $Ama2$, $P2_1/c$, $C2/c$, Pm, and $P\bar{1}$ as the only possible choices.

$P\bar{4}2_1c$ (D_{2d}^2) produces the weak 30.6° 2θ 201 peak. This space group has been reported for $(ND_4)_2TeCl_6$ (12), and this also gave a good description of the peaks observed at 5 K. $PdCl_6$ is free to rotate about the Z-axis only in this space group. The lowest χ^2 reached was 15.5, but the model was very unstable and would not converge.

$P4/m$, converged to a χ^2 of 17. Refinement in the space group $Cccm$ was relatively unstable and would not proceed below a χ^2 of 45. Ultimately, by such trials the choices were narrowed to two possible monoclinic space groups: $C2/c$ (C_{2h}^6) and $P2_1/n$ (C_{2h}^5). Both these space groups have been reported as possible low-temperature space groups in other antifluorite systems.

Refinement as $C2/c$ (C_{2h}^6)

The relationship of the atomic positions between the $C2/c$ and $Fm\bar{3}m$ lattices is

$$\begin{pmatrix} x \\ y \\ z \end{pmatrix} = \begin{pmatrix} 100 \\ 010 \\ 001 \end{pmatrix} \begin{pmatrix} x \\ y \\ z \end{pmatrix}_{Fm\bar{3}m} - \begin{pmatrix} 1/4 \\ 1/4 \\ 0 \end{pmatrix}. \quad (1)$$

In the 5 K refinements the rigid bodies were given the freedom to rotate and translate as allowed by symmetry, while preserving their undeformed molecular geometries. Bond lengths of the MX_6 and ND_6 molecular units were allowed to vary, but the bond lengths of the two symmetrically distinct ND_4 ions were constrained to be identical. Assuming the structure to be a small distortion of the cubic form, the T and L tensors were constrained to only one component each, and the rigid bodies were inserted into the monoclinic setting using starting orientations deduced from mapping $Fm\bar{3}m$ (O_h^5) onto $C2/c$ (C_{2h}^6). The fit with such initial orientations is very poor. The rotational degrees of freedom of the rigid molecules were then turned on one by one. Almost no improvement was found on initially varying the $PdCl_6$ orientation. The orientational parameters of the ND_4 ions were then varied. Large damping factors were used initially (90%). These factors were reduced in stages until they were removed entirely once the refinement became more stable with respect to these variables. The results of the refinement are shown in Table 4. Relatively large rotations were seen with respect to the ideal ⟨111⟩ orientations of the cubic phase. The rotations and translations quoted in these tables are with respect to the Cartesian system of the rigid body XYZ (25). Damping of these variables was gradually reduced. Finally temperature factors were refined for each rigid body type. It was found that the L component became an ill-defined variable and was unstable in the refinement, and so was fixed to $(0°)^2$. The final χ^2 was 6.1. The observed and fitted diffraction patterns are plotted in Fig. 3.

Refinement as $P2_1/n$ (C_{2h}^5)

The space group $P2_1/n$ (C_{2h}^5) is a lower symmetry than $C2/c$.

The relationship between $P2_1/n$ (unique axis y) and $Fm\bar{3}m$ may be expressed as

$$\begin{pmatrix} x \\ y \\ z \end{pmatrix}_{P2_1/n} = \begin{pmatrix} 110 \\ \bar{1}10 \\ 001 \end{pmatrix} \begin{pmatrix} x \\ y \\ z \end{pmatrix}_{Fm\bar{3}m}, \quad (2)$$

so that the x and y coordinates are rotated 45° with respect to the cubic phase.

The refinement process was similar to that of the $C2/c$ refinement, with one component T and L tensors and damped molecular rotations. Again, the L component was found to be unstable with respect to refinement, as was found in the refinement in $C2/c$ (C_{2h}^6). We believe that this is a "real" result and that the magnitude of the thermal librations are essentially zero at 5 K, since the refined libration at room temperature is only of the order of 1°. The refinement also proceeded well to a χ^2 value of 3.6. The results of the

TABLE 4
Structural Parameters for $(ND_4)_2PdCl_6$ at 5 K, Refined as $C2/c$ (C_{2h}^6)

a/Å	b/Å	c/Å	β/°	V/Å^3
9.7047(10)	9.7015(11)	9.8008(6)	89.94(1)	922.76(14)

Atom	x	y	z	T/Å^2	L/°^{2}	U_{iso}/Å^2
Pd	0.2500	0.2500	0.0000	0.0163(6)		0.0163
Cl	0.4888(3)	0.2389(5)	−0.0016(5)	0.0163(6)	0	0.0163
Cl	0.2611(5)	0.4888(3)	0.0010(6)	0.0163(6)	0	0.0163
Cl	0.2513(5)	0.2486(7)	0.2367(2)	0.0163(6)	0	0.0163
N	0.0000	0.4965(8)	0.2500	0.0258(1)		0.0258
D	−0.0833(4)	0.5553(8)	0.2491(8)	0.0258(1)	146(9)	0.0546
D	−0.0010(8)	0.4375(8)	0.3325(4)	0.0258(1)	146(9)	0.0546
N	0.0000	−0.0176(8)	0.2500	0.0258(1)		0.0258
D	−0.0712(6)	−0.0765(8)	0.2929(9)	0.0258(1)	146(9)	0.0546
D	0.0432(9)	0.0413(9)	0.3204(6)	0.0258(1)	146(9)	0.0546

Rigid unit orientation parameters for $(ND_4)_2PdCl_6$ refined as $C2/c$ (C^62h) at 5 K
(R_X, R_Y, R_Z are rigid body rotations around XYZ: $X \parallel a$, $Z \parallel a \times b$, and $Y \parallel (a \times b) \times a$)

Body	Bond/Å	R_X/°	R_Y/°	R_Z/°
ND_4 #1	0.984(4)	0.00	14.3(6)	0.00
ND_4 #2	0.984(4)	0.00	45.6(7)	0.00
$PdCl_6$	2.320(3)	−0.3(2)	−0.4(1)	2.7(1)

refinement are shown in Table 5. The characteristics of the refinement were similar to that of $C2/c$ (C_{2h}^6)—small rotations of the $PdCl_6$ octahedra and large rotations of the ND_4 tetrahedral units. The observed and fitted diffraction patterns are shown in Fig. 4.

CONCLUSIONS

We have shown that the cubic phase of $(ND_4)_2PdCl_6$ shows considerable off-axis tilting of the ND_4 molecule, similar to that reported by (19) in their study of $(ND_4)_2SeCl_6$. Our refinement of this disorder gives an angular deviation of $19 \pm 1°$ from the [111] direction. Whether the true nature of the disorder is a static, or dynamic site occupation, or a rather more continuous distributions of nuclear intensity, could probably only be determined from a symmetry-adapted harmonic fit. There are few ammonium compounds where this approach has been used (see (32, 33) and references therein). The harmonics study of the antifluorite $(NH_4)_2SnCl_6$ (33) has demonstrated the exist-

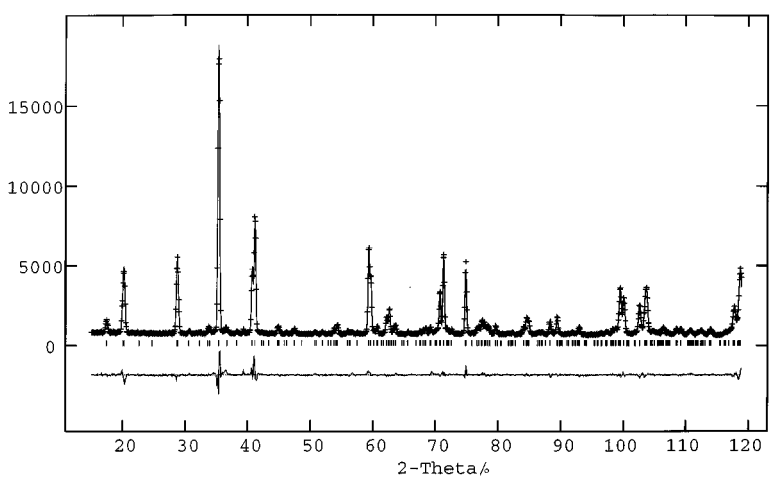

FIG. 3. Observed (points) and fitted (line) patterns of the diffraction pattern of $(ND_4)_2PdCl_6$ at 5 K, assuming symmetry $C2/c$ (C_{2h}^6).

TABLE 5
Structural Parameters for $(ND_4)_2PdCl_6$ Refined as $P2_1/n$ (C_{2h}^5) at 5 K

a/Å	b/Å	c/Å	β/°	V/Å^3
6.8569 (5)	6.8560 (5)	9.7938 (4)	90.06 (1)	460.41 (5) [920.82]

Atom	x	y	z	T/Å^2	L/°^{2}	U_{iso}/Å^2
Pd	0.0000	0.0000	0.0000	0.017(1)		0.017
Cl	0.2474(3)	0.2293(4)	−0.0005(4)	0.017(1)	0	0.017
Cl	0.2293(4)	−0.2474(4)	0.0035(4)	0.017(1)	0	0.017
Cl	−0.0025(5)	0.0042(6)	0.2361(2)	0.017(1)	0	0.017
N	0.5001(11)	0.0001(10)	0.2493(10)	0.029(1)		0.029
D	0.6441(14)	0.0244(13)	0.2645(14)	0.029(1)	91(6)	0.048
D	0.4552(22)	0.0739(19)	0.1654(16)	0.029(1)	91(6)	0.048
D	0.4770(13)	−0.1444(13)	0.2355(12)	0.029(1)	91(6)	0.048
D	0.4240(22)	0.0466(20)	0.3316(17)	0.029(1)	91(6)	0.048

Rigid Unit Orientation Parameters for $(ND_4)_2PdCl_6$ Refined as $P2_1/n$ (C_{2h}^5) at 5 K
(R_X, R_Y, R_Z are rigid body rotations around XYZ: $X \parallel a$, $Z \parallel a \times b$, and $Y \parallel (a \times b) \times a$)

Body	Bond/Å	R_X/°	R_Y/°	R_Z/°
ND_4	1.012(3)	26.9(5)	−23.5(6)	−5.6(7)
$PdCl_6$	2.313(2)	0.7(1)	0.5(1)	2.2(1)

Note. The volume in square brackets is given for comparison to the nonprimitive cubic and $C2/c$ cells.

ence of substantial disorder about the [111] direction in this compound, while maintaining a physically meaningful model of the NH_4 ion.

It is difficult to determine uniquely the space group of the low-temperature structure of $(ND_4)_2PdCl_6$ from the powder data. However, it has been possible to show that it is a pseudo-tetragonal monoclinic structure, crystallizing in either $C2/c$ or $P2_1/n$ space groups. Both 5 K refinements show that the molar volume increases below T_c, as was reported in the case of $(ND_4)_2TeCl_6$ (12). As pointed out by (12), it can be inferred from basic thermodynamics that these low-temperature phases are likely to be unstable with the application of pressure. It is also obvious from Figs. 5 and 6 that the chief effect of the phase transition is a rotation of the ND_4 units about an axis equivalent to [010] of the cubic phase.

The χ^2 of the $P2_1/n$ (C_{2h}^5) refinement is significantly lower than that of the $C2/c$ (C_{2h}^6) refinement. Crystal-chemical

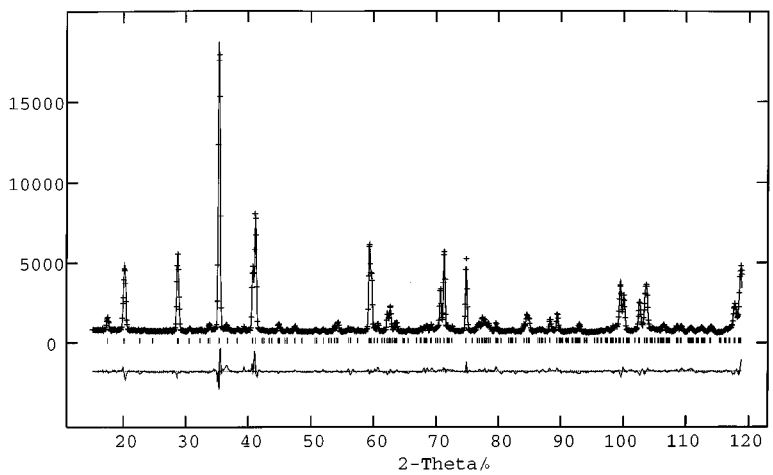

FIG. 4. Observed (points) and fitted (line) patterns of the diffraction pattern of $(ND_4)_2PdCl_6$ at 5 K, assuming symmetry $P2_1/n$ (C_{2h}^5).

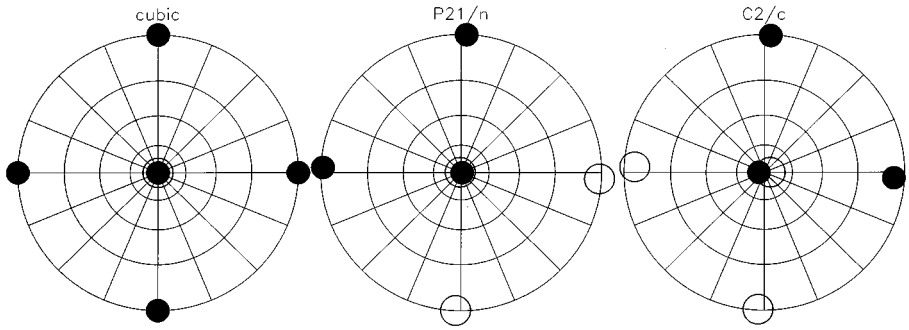

FIG. 5. Stereographic projection (pole figure) showing the orientation of the $PdCl_6$ octahedron located at [0, 0, 0] in the cubic phase. The figures are (from left to right) the cubic phase (along ⟨100⟩ directions), the $P2_1/n$ phase (rotated back to the cubic orientation), and the $C2/c$ phase. The closed circles represent Pd–Cl bond vectors with a positive component in z; the open circles represent Pd–Cl bond vectors with a negative component in z. It can be seen that in both monoclinic refinements the $PdCl_6$ octahedron undergoes very minor rotations during the phase transition.

arguments provide an additional means of choosing between the two possibilities. The value of the refined N–D bond length can be taken as a guide. In $C2/c$ (C_{2h}^6) the value was determined to be 0.984(4) Å, whereas in $P2_1/n$ (C_{2h}^5) the value was determined to be 1.012(3) Å. This latter value is closer to the 1.025(2) Å value given by Brown (27) as the mean N–D bond length of several different ND_4-compounds. Therefore, from both crystal-chemical and goodness-of-fit considerations we suggest that $P2_1/n$ (C_{2h}^5) is the space group for the compound at 5 K.

The monoclinic angle, β, is very close to 90°, but this is also true of other antifluorites that have been refined as monoclinic phases, e.g. $(NH_4)_2SnBr_6$ $\beta = 90.06(3)^\circ$ (1), and $(NH_4)_2PtI_6$ $\beta = 89.86(3)^\circ$ (2). In the antifluorites K_2TeBr_6, K_2SeBr_6 and K_2SnCl_6 where there are multiple transitions, $Fm\bar{3}m \rightarrow P4/mnc \rightarrow C2/c \rightarrow P2_1/n$, it has been pointed out

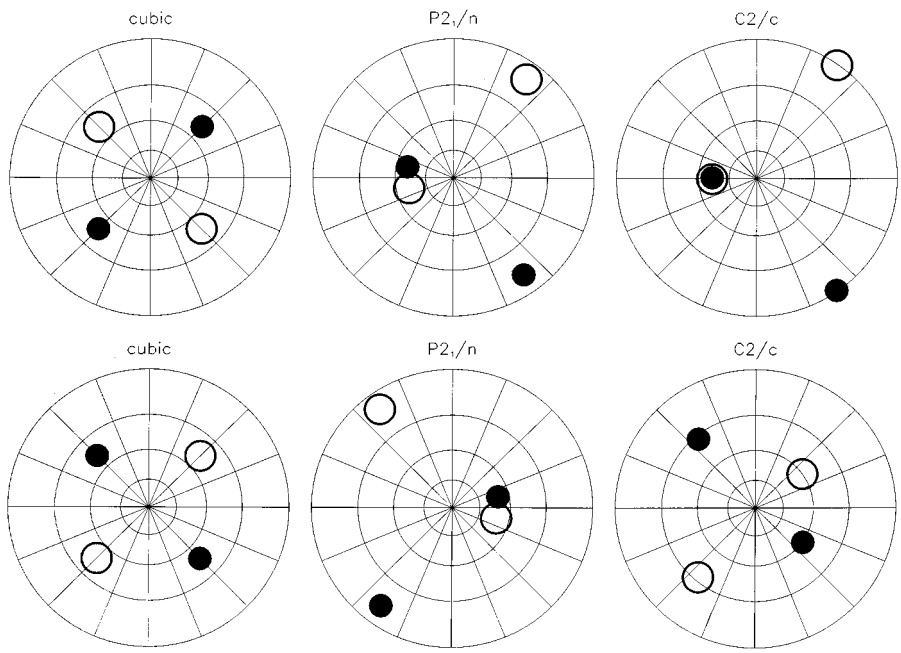

FIG. 6. Stereographic projection (pole figure) showing the orientation of the ND_4 tetrahedra in (from left to right) the cubic phase in the "normal" or ordered orientations (along ⟨111⟩ directions), the $P2_1/n$ phase (rotated back to the cubic orientation), and the $C2/c$ phase. The upper series are ND_4 tetrahedra located at [1/4, 3/4, 1/4] and the lower series at [1/4, 1/4, 1/4] in the cubic settings. The closed circles represent N–D bond vectors with a positive component in z; the open circles represent N–D bond vectors with a negative component in z. In $C2/c$ there are two symmetrically distinct ND_4 tetrahedra, whereas in the cubic phase and $P2_1/n$ setting there is only one symmetrically distinct tetrahedron. It can be seen that the ND_4 tetrahedra undergo major reorientations during the phase transition. Both monoclinic refinements show a similar geometrical orientation of the ND_4 ions, giving us some confidence in our interpretation of the nature of the transition.

that to lowest order the monoclinic angle may be forced to be 90° due to mode coupling between rotational modes of the MX_6 octahedra (10). In $(ND_4)_2PdCl_6$, however, it appears that the transition pathway occurs in one stage to the monoclinic space group from $Fm\bar{3}m$.

The largest change in the structure on cooling to 5 K in $(ND_4)_2PdCl_6$ is the large rotation of the ND_4 units (see Fig. 6). In contrast, while MX_6 rotational modes are usually considered to be the soft mode instabilities in these structures, the rotation of the $PdCl_6$ is almost insignificant (see Fig. 5). However, in the alkali metal antifluorite K_2OsCl_6 (29) the rigid body rotation of these groups is limited to the order of 2°, despite the soft mode being a librational MX_6 mode (7). In previous refinements of low-temperature protonanted ammonium antifluorites (e.g., (1–3)), the orientation of the ammonium ions in the low-temperature structures has not been refined, so it is not possible to suggest whether the large rotations of ND_4 observed in $(ND_4)_2PdCl_6$ are unusual. The dominance of the ND_4 molecular rotations should, perhaps, be expected in a compound where the transition is inhibited on protonation.

An examination of the calorimetric data available for deuterated-ammonium antifluorites which undergo isotope-dependent phase transitions that $(ND_4)_2PdCl_6$ may be an extreme case: the transition entropies, $\Delta_{trs}S^\circ_m$, are $1.216 \pm 0.004R$ and $2.005 \pm 0.009R$ for $(ND_4)_2PtCl_6$ (16) and $(ND_4)_2PdCl_6$ (14), respectively. $(ND_4)_2TeCl_6$ (22) shows three transitions with $\Delta_{trs}S^\circ_m$ of $0.234 \pm 0.006R$, $0.247 \pm 0.006R$, and $0.861 \pm 0.007R$. The sum of these three transition entropies is $1.342R$, roughly comparable to that of $(ND_4)_2PtCl_6$. The entropy of the transition in $(ND_4)SeCl_6$ (20) has been reported as $1.455R$ (19, 20).

It would appear from our measurements of the magnitude of the librations in the cubic phase, and the relative magnitude of the ND_4 and $PdCl_6$ reorientations in the low-temperature phase that the majority of this entropy is associated with the ND_4 reorientations. Examining these entropies in terms of mol ND_4, gives us a comparison between the isotopically induced transitions in these compounds. In increasing order, the value of $\Delta_{trs}S^\circ_m$ for $(ND_4)_2MCl_6$ are $R \ln 1.84\,mol^{-1}$ ND_4, $R \ln 1.96\,mol^{-1}$ ND_4, $R \ln 2.07\,mol^{-1}$ ND_4 and $R \ln 2.73\,mol^{-1}$ ND_4, where M = Pt, Te, Se, and Pd, respectively. All four compounds suggest an order–disorder relationship, as $\Delta_{trs}S^\circ_m \gtrapprox R \ln 2\,mol^{-1}$ ND_4, between the low-temperature and cubic phases, but clearly the Pd-compound stands out as the extreme case. The activation energy for classical reorientation of NH_4^+ in $(NH_4)_2PdCl_6$ is the lowest known of all the $(NH_4)_2MCl_6$ salts (30, 31). In addition, the quantum tunneling frequency shows an exponential increase with the lattice parameter, a, in $(NH_4)_2MCl_6$ salts increasing from $M = Te^{4+}$, to Pb^{4+}, Sn^{4+}, and Pd^{4+} (14, 30). $(NH_4)_2PdCl_6$, therefore, has the lowest known barrier to both classical and quantum ammonium reorientation. If we assume that $(ND_4)_2PdCl_6$ is at a similar extreme in the $(ND_4)_2MCl_6$ salts, this may explain the high $\Delta_{trs}S^\circ_m$ associated with the ordering transition in this compound.

ND_4 disorder has been reported in structural studies of $(ND_4)_2SeCl_6$ (19) suggesting that this is indeed a common feature of the cubic ammonium antifluorites. The fact that all of these transitions, which are potentially classifiable as order–disorder, show quite different transition entropies, indicates that a simple model of 1/3 occupancy of the 96k sites in the disordered form, ordering to a single orientation in the low-temperature phase is probably too simple. It is probable that a continuous D-nuclear density distribution about [111] exists, with each compound having a different amplitude, dependent upon the case of ammonium reorientation.

The analysis of the room-temperature inelastic spectrum of the cubic protonated analogue, $(NH_4)_2PdCl_6$, assumed that the scattering from the librational motion of the NH_4 ion dominated the inelastic spectrum on the basis of the relatively large total scattering cross-section of H and relatively low inertia of NH_4 (6). The extremely small librational amplitude of the $PdCl_6$ unit refined in the deuterated cubic phase suggests that this assumption is correct.

ACKNOWLEDGMENTS

We thank Dr. M. Prager (Jülich) for providing the sample for this study and Ron Donaberger (McMaster University) for expert technical help. We also thank the reviewers for their constructive comments.

REFERENCES

1. R. L. Armstrong, R. M. Morra, B. M. Powell, and W. J. L. Buyers, *Can. J. Phys.* **61,** 997 (1983).
2. M. Sutton, R. L. Armstrong, B. M. Powell, and W. J. L. Buyers, *Can. J. Phys.* **59,** 449 (1981).
3. R. L. Armstrong, B. Lo, and B. M. Powell, *Can. J. Phys.* **67,** 1040 (1989).
4. H. Boysen and A. W. Hewatt, *Acta Crystallogr. Sect. B* **34,** 1412 (1978).
5. H. Boysen, J. Ihringer, W. Prandl, and W. Yelon. *Solid State Commun.* **20,** 1019 (1976).
6. M. Prager, W. Press, A. Heidemann, and C. Vettier, *J. Chem. Phys.* **80,** 2777 (1983).
7. M. Sutton, R. L. Armstrong, B. M. Powell, and W. J. L. Buyers, *Can. J. Phys.* **69,** 380 (1983).
8. B. M. Powell, W. Press, and G. Dolling, *Phys. Rev. B* **32,** 3118 (1985).
9. J. M. Zhang, W. Lu, S. C. Shen, Y. C. Xu, and J. Pelzl, *J. Phys. Soc. Jpn.* **64,** 2913 (1995).
10. J. Ihringer and S. C. Abrahams, *Phys. Rev. B* **30,** 6540 (1984).
11. R. L. Armstrong, R. M. Morra, and B. M. Powell, *Can. J. Phys.* **63,** 988 (1985).
12. Y. Kume, Y. Miyazaki, T. Matsuo, H. Suga, W. I. F. David, and R. M. Ibberson, *Europhys. Lett.* **16,** 265 (1991).
13. J. E. Callanan, R. D. Weir, and E. F. Westerum, *J. Chem. Thermodyn.* **24,** 1001 (1992).
14. J. E. Callanan, R. D. Weir, and E. F. Westrum, *Ber. Bunsenges. Phys. Chem.* **96,** 1585 (1992).
15. R. D. Weir and E. F. Westrum, Jr., *J. Chem. Thermodyn.* **22,** 1097 (1990).

16. R. D. Weir and E. F. Westrum, Jr., *J. Chem. Thermodyn.* **23,** 653 (1991).
17. Y. Kume and T. Asaji, *J. Mol. Struct*. **345,** 145 (1995).
18. H. Muraoka, T. Matsuo, and Y. Kume, *Solid State Commun.* **93,** 529 (1995).
19. O. Yamamuro, H. Muraoka, T. Ohta, T. Matsuo, Y. Kume, N. Onoda-Yamamuro, K. Oikawa, and T. Kamiyama, *J. Phys. Soc. Jpn.* **64,** 2722 (1995).
20. Y. Kume, H. Muraoka, T. Matsuo, and H. Suga, *J. Chem. Thermodyn.* **26,** 211 (1994).
21. J. E. Callanan, R. D. Weir, and E. F. Westrum, *J. Chem. Thermodyn.* **22,** 567 (1990).
22. J. E. Callanan, R. D. Weir, and E. F. Westrum, *J. Chem. Thermodyn.* **24,** 661 (1992).
23. Y. Kume, Y. Miyazaki, T. Matsuo, H. Suga, *J. Phys. Chem. Solids* **53,** 1297 (1992).
24. M. Krupski. *Phys. Status Solids A* **116,** 657 (1989).
25. A. C. Larson and R. B. von Dreele, "LAUR 86-748," Los Alamos National Laboratory, Los Alamos, NM.
26. R. L. Armstrong, P. Dufort, and B. M. Powell, *Can. J. Phys.* **69,** 137 (1991).
27. R. J. C. Brown. *J. Mol. Struct*. **345,** 77 (1995).
28. H. T. Stokes and D. M. Hatch, Isotropy Subgroups of the 230 Crystallographic Space Groups", World Scientific, Singapore/New Jersey London/Hong Kong, 1988.
29. R. L. Armstrong, R. M. Morra, I. Svare, and B. M. Powell, *Can. J. Phys.* **65,** 386 (1987).
30. M. Prager, A. M. Raaen, and I. Svare, *J. Phys. C Solid State Phys.* **16,** L181 (1983).
31. I. Svare, A. M. Raaen, and G. Thorkildsen, *J. Phys. C. Solid State Phys.* **11,** 4069 (1978).
32. J. Rubín, E. Palacios, J. Bartolemé, and J. Rodríguez-Caravajal, *J. Phys Condens. Matter* **7,** 563 (1995).
33. K. Vogt and W. Prandl, *J. Phys. C Solid State Phys.* **16,** 4753 (1993).